

Supporting informations

Cationic redistribution at epitaxial interfaces in superconducting two-dimensionally doped lanthanum cuprate films

Federico Baiutti, Giuliano Gregori, Yi Wang, Y. Eren Suyolcu, Georg Cristiani, Peter A. van Aken, Joachim Maier and Gennady Logvenov.*

Max Planck Institute for Solid State Research, Heisenbergstr. 1, 70569 Stuttgart, Germany

E-mail: fbaiutti@irec.cat

Contents

Figure S1. Representative EELS and EDXS linescans for Sr, Ca and Ba two-dimensionally doped La_2CuO_4 .

Figure S2. AFM micrographs for Ca and Ba two-dimensionally doped La_2CuO_4 .

Figure S3. R vs T for two dimensionally Dy-doped La_2CuO_4 .

Figure S4. Large HAADF image for two-dimensionally Dy-doped La_2CuO_4 .

Figure S5. Large area HAADF image and representative EDXS linescan for two-dimensionally Sr-doped La_2CuO_4 .

Figure S6. Fitting of the experimental Sr concentration profile.

Note S1. Details on the fitting of the experimental Sr concentration profile.

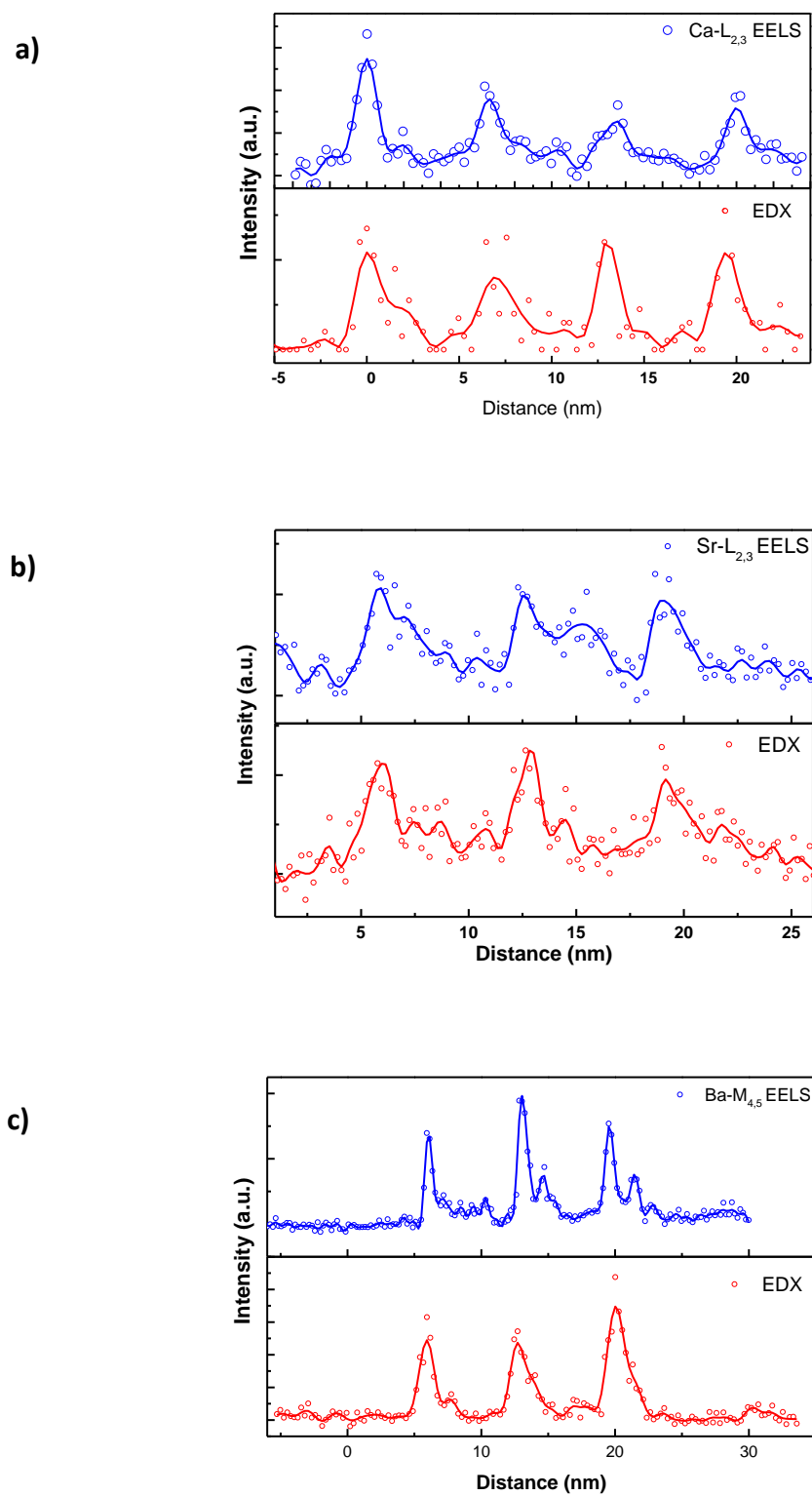


Figure S1. Representative EELS and EDXS linescans for Ca (a), Sr (b) and Ba (c) two-dimensionally doped La_2CuO_4 .

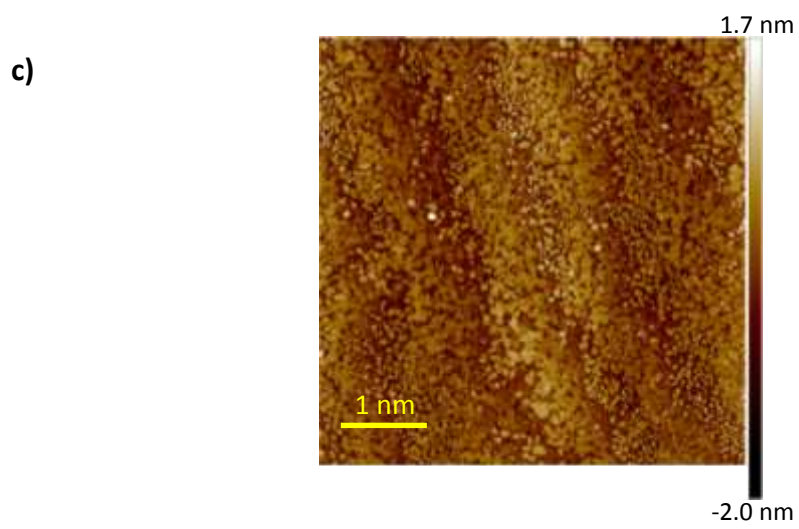
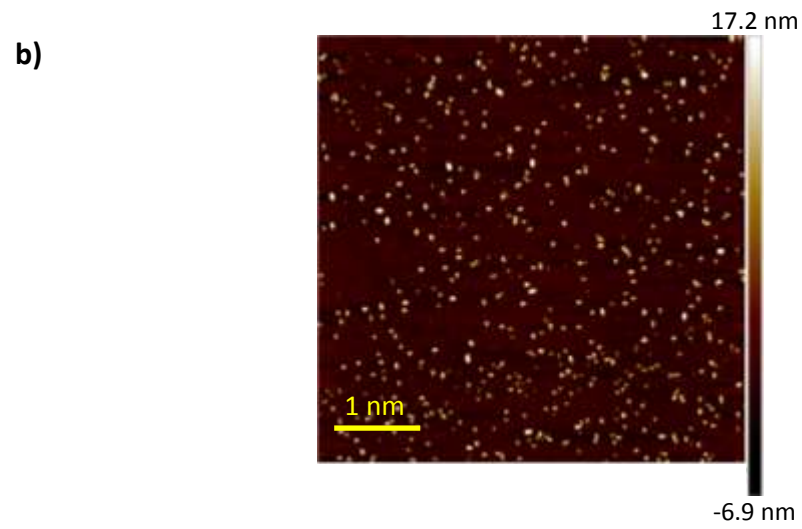
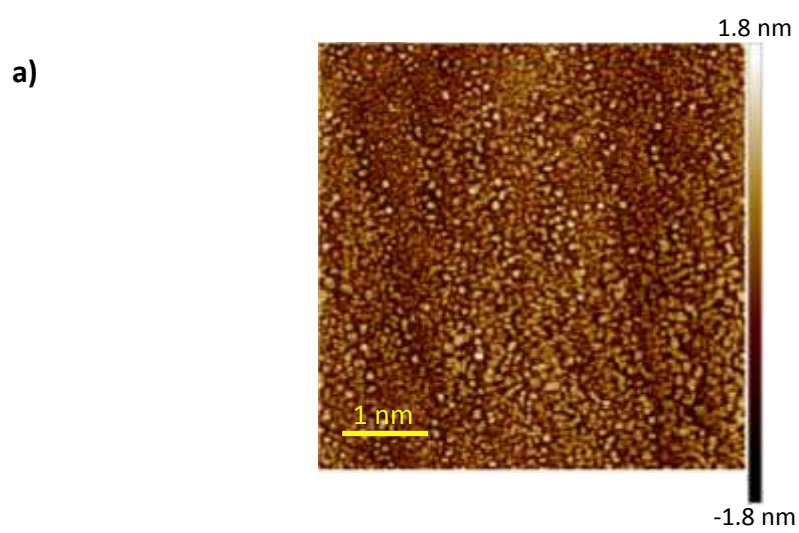


Figure S2. AFM micrographs for Ca (a - R_{ms} roughness 0.55 nm) and Ba (b - $R_{\text{ms}} = 2.65$ nm and c - $R_{\text{ms}} = 0.59$ nm) two-dimensionally doped La_2CuO_4 . One can notice a high tendency to secondary phase formation in the case of Ba-doping (b). Only by adjusting the Cu stoichiometry for each layer during the growth and by reducing the final sample thickness, the presence of such precipitates can be limited, as demonstrated by the micrograph shown in (c). For the AFM analysis of the Sr-doped case please refer to Ref. 13.

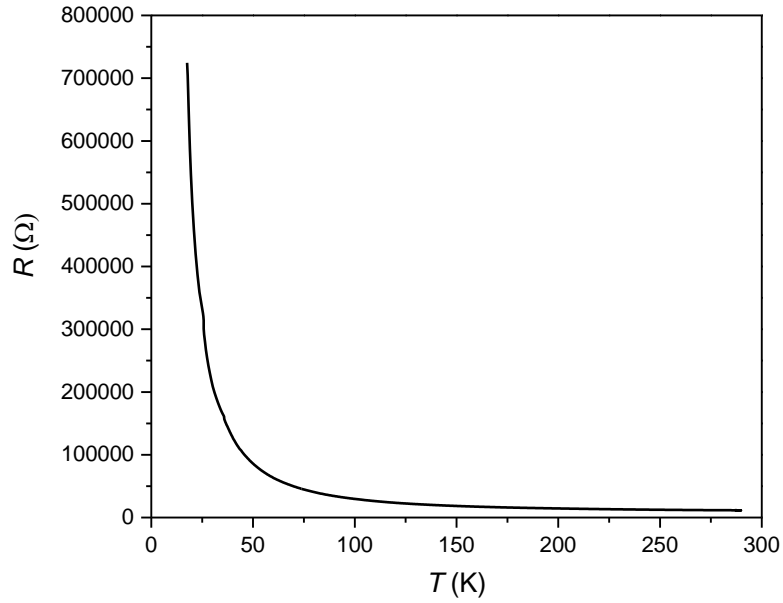


Figure S3. R vs T for two dimensionally doped La_2CuO_4 having formula $3 \times (\text{Dy}_{0.5}\text{La}_{0.5}\text{O}-\text{LaO}-\text{CuO}_2) + 9 \times \text{LaO}-\text{LaO}-\text{CuO}_2$.

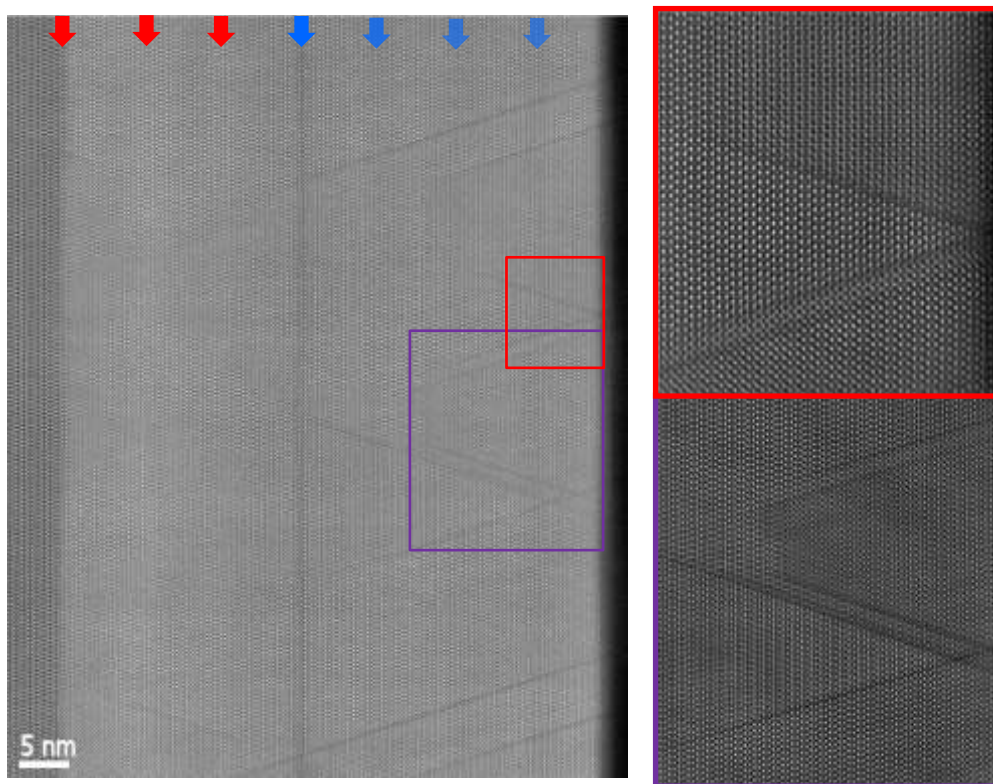


Figure S4. Large area HAADF image for two-dimensionally doped La_2CuO_4 having the following composition:

$$3 \times [\text{La}_{1.5}\text{Dy}_{0.5}\text{CuO}_4 + 9 \times \text{La}_2\text{CuO}_4] + \\ [\text{SrO-LaO-CuO}_4 + 9 \times \text{La}_2\text{CuO}_4] + 3 \times [\text{La}_{1.5}\text{Sr}_{0.5}\text{CuO}_4 + 9 \times \text{La}_2\text{CuO}_4]$$

The red and blue arrows indicate the Dy and Sr doped regions, respectively. The presence of some extended defects, originating from the Dy-doped area, can be observed.

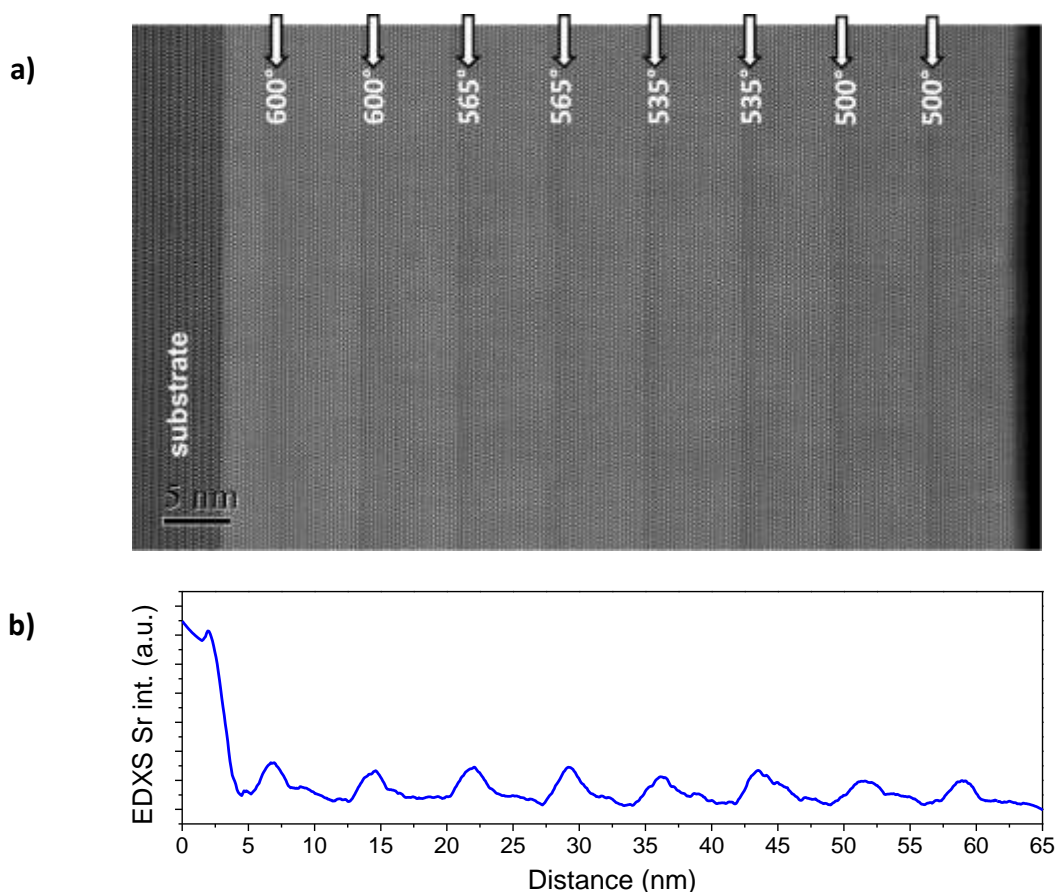


Figure S5. a) Large area HAADF image for Sr two-dimensionally doped La_2CuO_4 , in which the doped areas have been deposited at progressively decreasing temperatures. b) EDXS linescan in the growth direction.

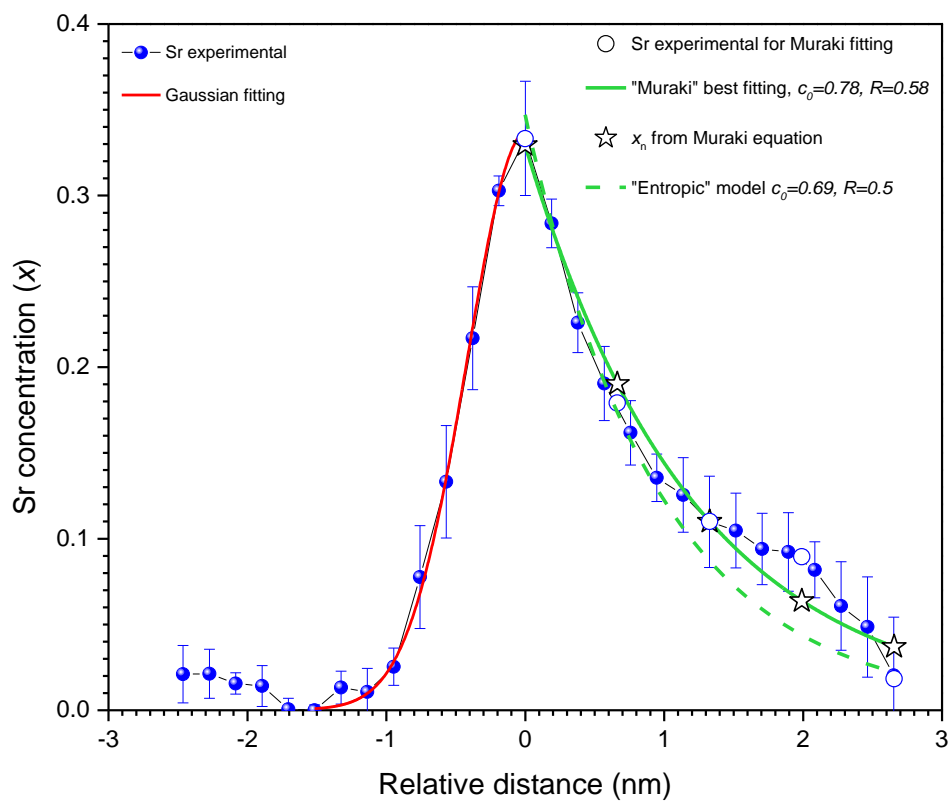


Figure S6. Fitting of the experimental Sr concentration profile (see also Supplementary Note 1).

Note S1

For the fitting of the Sr distribution at the downward interface side, the following Gaussian equation has been employed:

$$c = \frac{A}{\sigma\sqrt{2\pi}} \exp\left(-\frac{1}{2}\left(\frac{z}{\sigma}\right)^2\right)$$

With c being the concentration, A the curve integral, σ the standard deviation of the distribution and z the spatial coordinate. The fitting was operated by Origin Software, providing the final values (including the standard errors):

Adjusted res.-square	0.998
σ	0.430±0.033
A	0.364±0.045

The total area under the experimental graph was calculated as 0.177±0.494, which is in very good agreement with the value of $A/2$ stemming from the fitting.

For what concerns the upward interface side, given the discrete character of the Muraki equation, the experimental values to be fitted (shown as empty blue circles in Supplementary Figure S6) were chosen as the Sr concentration experimental values having a spacing of 0.66 nm (i.e. the thickness of a single (La,A)O – (La,A)O – CuO₂ constituting block) between each other (when no experimental values were available with such a spacing, the linear regression between two neighboring points has been considered). The total Sr concentration $x_{0,exp} = 0.73\pm0.13$ was obtained as a sum of such intensities. These experimental data has been fitted using the Muraki equation:

$$x_n = x_0(1 - P)P^{n-1}$$

Which expresses the concentration x_n of each n -th block as a function of the nominal Sr concentration x_0 and of the segregation probability P . The resulting values of x_n (empty stars) and the best fitting curve (solid green line - $x_0 = 0.78$, $P = 0.59$, adjusted res.-square = 0.97) are reported in Supplementary Figure S6. For the fitting procedure, the following constraints were imposed in order to respect the nominal Sr stoichiometry: $0.6 \leq x_0 \leq 0.86$. The Sr profile stemming from the “entropic” model as described in the main text (dotted green line in Supplementary Figure S6) has been obtained by applying the following constraints: $0.6 \leq x_0 \leq 0.86$, $P = 0.50$. The resulting adjusted res.-square in this case is 0.95.